Density-of-states and partial-density-of-states functions for the cubic *d*-band perovskites

T. Wolfram and Ş. Ellialtioglu*
Department of Physics and Astronomy, University of Missouri, Columbia, Columbia, Missouri 65211
(Received 22 October 1981)

The electronic density-of-states and the partial-density-of-states functions for the 14 primary bands of the ABO_3 cubic *d*-band perovskites are derived as simple, closed form, analytical formulas with the use of an empirical linear-combinations-of-atomic-orbitals model. Comparisons of the model density functions with those derived from more accurate energy-band calculations presented for $SrTiO_3$, $KTaO_3$, and $NaWO_3$ are shown to be in good agreement.

I. INTRODUCTION

The DOS (density of states) and PDOS (partial density of states) functions are of fundamental importance in characterizing the electronic properties of solids and for qualitatively analyzing optical, photoelectron, transport, and other types of experimental data. The purpose of this paper is to provide simple, but reasonably accurate, analytical expressions for both the DOS and PDOS functions of the large class of cubic transition-metal oxides known as the "*d*-band perovskites."

The structure of the cubic perovskites is illustrated in Fig. 1. The formula unit is ABO_3, where *B* represents a 3*d*, 4*d*, or 5*d* transition-metal ion, O is an oxygen ion, and *A* is a group I*A*, II*A*, or II*B* metal ion. Well-known perovskites include insulators such as $SrTiO_3$, $BaTiO_3$, and $KTaO_3$, as well as metals such as $KMoO_3$, $NaWO_3$, and ReO_3.

Investigations of the electronic,[1–9] optical,[10,11] and photoelectron[11–17] properties of the perovskites have been discussed recently and there is a considerable amount of interest in developing theoretical models to interpret experimental data on the perovskites. The density functions including the DOS, JDOS (joint density of states), and PDOS are of fundamental importance in the interpretation of experimental data in terms of the energy bands of these solids. More complete discussions of the general properties of the perovskites can be found in Refs. 1, 2, and 18 and no attempt will be made here to review this information in detail.

The nonmagnetic perovskites appear to be properly described by convential one-electron energy-band theory even though polaron and correlation effects are undoubtedly very important.[3,18] In this paper we are concerned with the development of approximate analytical expressions for the density functions and we shall limit our considerations to perovskites for which energy-band theory is appropriate.

We employ the simple LCAO (linear combination of atomic orbitals) model that we have previously developed and that has been shown to correctly describe the 14 primary valence and conduction bands of the perovskites.[2,7] The LCAO model

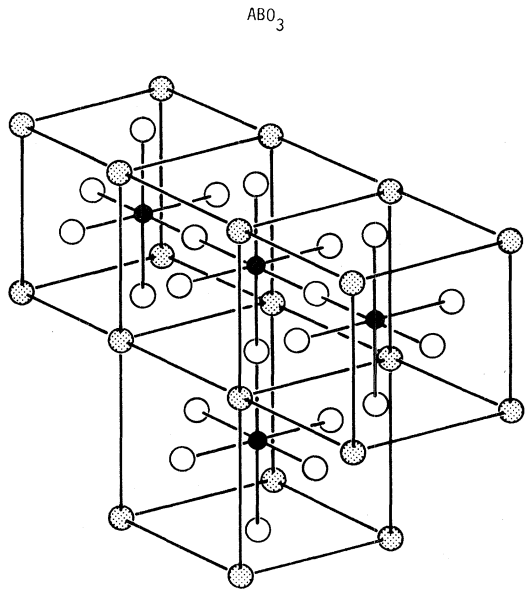

FIG. 1. Lattice structure of the ABO_3 cubic perovskite. The open circles represent oxygen ions, the solid circles indicate the transition-metal *B* ions and the shaded circles indicate the *A* ions. The lattice parameter is $2a$ where a is the *B*-O ion internuclear distance.

may be viewed as an interpolation scheme for describing the energy bands, as originally suggested by Slater and Koster,[19] or as an energy-band scheme for calculating the electronic properties qualitatively. The appropriate point of view depends upon whether one treats the parameters as adjustable or calculates them.

In Sec. II we briefly review the LCAO model results for the energy bands of the d-band perovskites. Section III is devoted to the details of the calculation of the DOS and PDOS functions. Results are obtained as simple analytical expressions that can easily be applied to an arbitrary d-band perovskite.

Some of the results for the DOS functions have been briefly described in previous[9,17] papers. Here we give a more complete discussion of the density functions and treat a somewhat more general model which includes the dispersion of the nonbonding oxygen valence bands.

Section IV presents comparisons of the analytical results derived here with numerical results obtained by other authors from their energy band calculations. A brief summary is given in Sec. V.

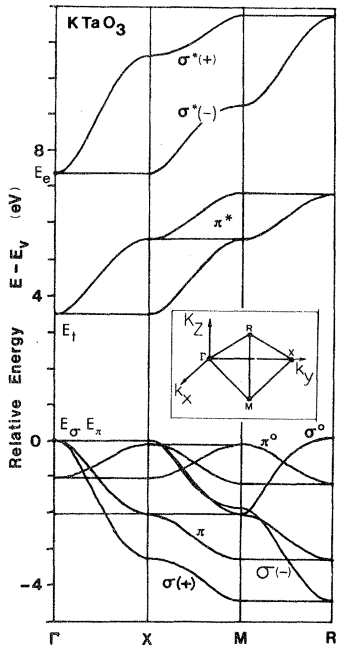

FIG. 2. Bulk energy bands for $KTaO_3$ using the LCLO model. The parameters employed are $E_\pi=0.0$, $E_t=3.5$ $(pd\pi)=1.68$, $(pd\pi)=0.23$, $E_\sigma=-2.05$, $E_e=7.35$, $(pd\sigma)=-2.95$, $(pp\sigma)=-0.3$ (all in eV). The parameters were determined by fitting the numerical results for the DOS and $KTaO_3$ of Ref. 7.

II. ENERGY-BAND MODEL FOR THE PEROVSKITES

In several previous works[2,17] we developed a simple model for the energy bands of the cubic perovskites using the LCAO approach. In this section we briefly review the results of the model.

The unit cell for the cubic ABO_3 perovskites is shown in Fig. 1. The B site is occupied by a transition-metal ion such as Ti, V, Nb, Mo, W, or Re; and the A site contains another (nontransition metal) cation such as an alkali-metal ion or Ca, Sr, Ba, or La. The energy bands of importance are the conduction and valence bands associated with the B and O ions. These bands, referred to as the primary energy bands, are illustrated in Fig. 2. The bands associated with the outer valence orbitals of the A ions occur at higher energies and will be omitted in our discussions.

Considering only the BO_3 part of the ABO_3 unit cell there are 14 basis orbitals to consider; the five nd orbitals of the B ions and three $2p$ orbitals of each of the three oxygen ions. Thus there will be 14 primary energy bands.

The wave functions are assumed to be of the form

$$\Psi_{\vec{k}}(r)=\sum_j\sum_m\sum_q c_{jq}^{\vec{k}\nu}\exp(i\vec{k}\cdot\vec{R}_{mj})\psi_q(\vec{r}-\vec{R}_{mj}) , \tag{1}$$

where $c_{jq}^{\vec{k}\nu}$ is the amplitude of the orbital $\psi_q(\vec{r}-\vec{R}_{mj})$ ($q=2p$, or nd) that is localized at the lattice position $\vec{R}_{mj}=\vec{R}_m-\vec{t}_j$ for the state whose wave-vector and band index are $\vec{k}$ and ν, respectively. The vector $\vec{R}_m$ is the position of the mth unit cell and $\vec{t}_j$ locates the jth ion within the mth unit cell. Instead of atomic orbitals we choose the localized functions ψ_q to be Löwdin orbitals[20] (orthogonalized atomic orbitals) so that the overlap matrix is diagonal;

$$\int\psi_{q'}(\vec{r}-\vec{R}_{m'j'})^*\psi_q(\vec{r}-\vec{R}_{mj})d\vec{r}=\delta_{jj'}\delta_{mm'}\delta_{qq'} , \tag{2a}$$

$$\sum_{jq}|c_{jq}|^2=1 . \tag{2b}$$

The eigenvectors and eigenvalues are easily calculated if the transfer integrals,

$$\int\psi_{q'}(\vec{r}-\vec{R}_{m'j'})^*H\psi_q(\vec{r}-\vec{R}_{mj})d\vec{r} , \tag{3}$$

are known (where H is the effective one-electron

Hamiltonian).

Previous studies[1,2,7,17] have shown that an excellent representation of the perovskite energy bands is obtained by retaining only the nearest-neighbor cation-anion interactions. In what follows, we consider both the first- (cation-anion) and second- (anion-anion) neighbor interactions.

A. π valence and conduction bands

There are three sets of symmetry-equivalent conduction and valence bands denoted by $\pi(\alpha\beta)$ and $\pi(\alpha\beta)^*$, respectively, where $\alpha\beta=xy$, xz, or yz. The energy-band dispersion is given by:

$$E_{\vec{k}\,\pi(\alpha\beta)}=\tfrac{1}{2}(E_\pi+E_t) -\{[\tfrac{1}{2}(E_\pi-E_t)]^2 +4(pd\pi)^2(S_\alpha^2+S_\beta^2)\}^{1/2}, \quad (4)$$

$$E_{\vec{k}\,\pi(\alpha\beta)^*}=\tfrac{1}{2}(E_\pi+E_t) +\{[\tfrac{1}{2}(E_\pi-E_t)]^2 +4(pd\pi)^2(S_\alpha^2+S_\beta^2)\}^{1/2}, \quad (5)$$

where $S_\alpha=\sin(k_\alpha a)$ and $2a$ is the lattice parameter. The energies E_π and E_t, the valence- and conduction-band-edge energies, are shown in Fig. 2. The quantity $(pd\pi)$ is the π-type transfer integral[19] between an oxygen $2p$ orbital and a $t_{2g}(xy)$ nd orbital.

The corresponding wave functions have the amplitudes:

$$c_{\begin{bmatrix}\alpha\\ \beta\end{bmatrix}}^{\vec{k}\,\pi(\alpha\beta)}=2iS_{\begin{bmatrix}\alpha\\ \beta\end{bmatrix}}(pd\pi)/D^{\pi(\alpha\beta)}, \quad (6)$$

$$c_{\alpha\beta}^{\vec{k}\,\pi(\alpha\beta)}=(E_{\vec{k}\,\pi(\alpha\beta)}-E_\pi)/D^{\pi(\alpha\beta)}, \quad (7)$$

$$c_{\begin{bmatrix}\alpha\\ \beta\end{bmatrix}}^{\vec{k}\,\pi(\alpha\beta)^*}=2iS_{\begin{bmatrix}\alpha\\ \beta\end{bmatrix}}(pd\pi)/D^{\pi(\alpha\beta)^*}, \quad (8)$$

$$c_{\alpha\beta}^{\vec{k}\,\pi(\alpha\beta)^*}=(E_{\vec{k}\,\pi(\alpha\beta)^*}-E_\pi)/D^{\pi(\alpha\beta)^*}, \quad (9)$$

$$D^\gamma=[(E_{\vec{k}\,\gamma}-E_\pi)^2 +4(pd\pi)^2(S_\alpha^2+S_\beta^2)]^{1/2}, \quad (10)$$

$$\gamma=\pi(\alpha\beta) \text{ or } \pi(\alpha\beta)^*. \quad (11)$$

In Eq. (6), $c_{\alpha\beta}^{\vec{k}\,\gamma}$ is the amplitude of the $t_{2g}(\alpha\beta)$ orbital and $c_\alpha^{\vec{k}\,\gamma}$ is the amplitude of the oxygen $2p(\alpha)$ orbital for the band state (k,γ).

The Brillouin zone for the perovskite structure is shown in the inset of Fig. 2 where the high-symmetry points labeled Γ, X, M, and R are indicated. The wave functions for the π (and π^*) bands are composed of only $2p$ (nd) orbitals at Γ. The admixture of nd and $2p$ orbitals increases away from Γ becoming a maximum at R, the corner of the zone.

B. π nonbonding bands

There are three equivalent nonbonding bands whose wave functions are composed entirely of oxygen $2p$ orbitals. For the nearest-neighbor approximation these bands are "flat"; that is, without dispersion. The energy and wave-function amplitudes are the following:

$$E_{\vec{k}\,\pi^0(\alpha\beta)}=E_\pi, \quad (12)$$

$$c_{\alpha\beta}^{\vec{k}\,\pi^0(\alpha\beta)}=0, \quad (13)$$

$$c_\alpha^{\vec{k}\,\pi^0(\alpha\beta)}=S_\beta/(S_\alpha^2+S_\beta^2)^{1/2}. \quad (14)$$

If the second-neighbor (oxygen-oxygen) interactions are added to the model then to an excellent approximation the only significant change in the energy bands is to replace the $\pi^0(\alpha\beta)$ band energy of Eq. (11) by

$$E_{\vec{k}\,\pi^0(\alpha\beta)}=E_\pi-4(pp\pi)C_\alpha^2C_\beta^2 +2[(pp\sigma)-(pp\pi)]S_\alpha^2S_\beta^2, \quad (15)$$

where $(pp\pi)$ and $(pp\sigma)$ are the oxygen π and σ integrals between $2p$ orbitals[2,19] and $C_\alpha=\cos(k_\alpha a)$. The energy given in Eq. (15) is exact at Γ, X, M, and R and is an excellent interpolation formula for all k in the Brillouin zone. The effect of the oxygen-oxygen interactions on the π and π^* bands is very minor and can be neglected.

C. σ valence and conduction bands

For the simple, nearest-neighbor interaction model, there is no coupling between the π and σ bands and they may be considered independently. The nearest-neighbor model gives an excellent representation of the p-d conduction and valence bands of the perovskites, but leads to flat (i.e., without dispersion) nonbonding oxygen valence bands.[1] The addition of second-neighbor interactions (the oxygen-oxygen interactions) produces the energy-band dispersion of the nonbonding bands. For this second-neighbor model it is found that the effect of the oxygen-oxygen interactions on the p-d valence and conduction bands is very minor be-

cause of the smallness of the LCAO oxygen-oxygen transfer integrals compared to the *p-d* integrals and the fact that only off-diagonal matrix elements are involved. Consequently, the very weak coupling between the π and σ bands that is introduced when second-neighbor interactions are included can be ignored without significantly altering any important features of the perovskite bands. In the work reported here we include the effects of the oxygen-oxygen interactions on the dispersion of the nonbonding bands but neglect such effects on the *p-d* conduction and valence bands.

For the σ-type bands there are two inequivalent valence bands and two inequivalent conduction bands denoted by $\sigma(\pm)$ and $\sigma^*(\pm)$, respectively. The energies are given by

$$E_{\vec{k}\sigma^*(\pm)}=\tfrac{1}{2}(E_e+E_\sigma)+\{[\tfrac{1}{2}(E_e-E_\sigma)]^2+2(pd\sigma)^2(S_x^2+S_y^2+S_z^2\pm S^2)\}^{1/2}, \tag{16}$$

$$E_{\vec{k}\sigma(\pm)}=\tfrac{1}{2}(E_e+E_\sigma)-\{[\tfrac{1}{2}(E_e-E_\sigma)]^2+2(pd\sigma)^2(S_x^2+S_y^2+S_z^2\pm S^2)\}^{1/2}, \tag{17}$$

$$S^2=(S_x^4+S_y^4+S_z^4-S_x^2S_y^2-S_x^2S_z^2-S_y^2S_z^2)^{1/2} \qquad (S_\alpha=\sin\vec{k}_\alpha a). \tag{18}$$

In Eqs. (16) and (17) the parameter $(pd\sigma)$ is the transfer integral[19] between an $e_g(3z^2-r^2)$ *nd* orbital and a $2p(z)$ oxygen orbital. The parameters E_σ and E_e are the band-edge energies for the σ and σ^* bands at Γ in the Brillouin zone, respectively. An illustration of these σ bands is shown in Fig. 2.

The wave-function amplitudes are the following:

$$c_{z^2}^{\vec{k}\nu}=\frac{(E_\sigma-E_{\vec{k}\nu})X^\nu}{(pd\sigma)\Delta^{\vec{k}\nu}}, \tag{19}$$

$$c_z^{\vec{k}\nu}=2iS_zX^\nu/\Delta^{\vec{k}\nu}, \tag{20}$$

$$c_{x^2}^{\vec{k}\nu}=-3(E_\sigma-E_{\vec{k}\nu})\frac{(S_x^2-S_y^2)}{(pd\sigma)\Delta^{\vec{k}\nu}}, \tag{21}$$

$$c_x^{\vec{k}\nu}=-\frac{iS_xX^\nu+3(S_x^2-S_y^2)}{\Delta^{\vec{k}\nu}}, \tag{22}$$

$$c_y^{\vec{k}\nu}=-\frac{iS_yX^\nu-3(S_x^2-S_y^2)}{\Delta^{\vec{k}\nu}}, \tag{23}$$

$$\Delta^{\vec{k}\nu}=(X^\nu)^2\left[\frac{(E_\sigma-E_{\vec{k}\nu})^2}{(pd\sigma)^2}+S_x^2+S_y^2+4S_z^2\right]+3(S_x^2-S_y^2)^2\left[\frac{(E_\sigma-E_{\vec{k}\nu})}{(pd\sigma)^2}+6\right], \tag{24}$$

$$X^\nu=\frac{[(E_\sigma-E_{\vec{k}\nu})(E_e-E_{\vec{k}\nu})-3(pd\sigma)^2(S_x^2+S_y^2)]}{(pd\sigma)^2},$$

$\nu=\sigma(\pm)$ or $\sigma^*(\pm)$.

The amplitudes $c_{z^2}^{\vec{k}\nu}$ and $c_{x^2}^{\vec{k}\nu}$ are for the $d(3z^2-r^2)$ and $d(x^2-y^2)$ orbitals, respectively, on the *B* ion. The amplitudes $c_\alpha^{\vec{k}\nu}$ ($\alpha=x$, y, or z) refer to the $2p$ oxygen orbital which is located a distance a along the αth coordinate axis from the *B* ion.

It can easily be shown that at Γ the $\sigma^*(\pm)$ wave functions have only e_g type ($3z^2-r^2$ or x^2-y^2) orbitals with nonzero amplitudes. Similarly, at $\vec{\Gamma}$ and $\sigma(\pm)$ wave functions have only $2p$-orbital amplitudes. Mixing of the *nd* and $2p$ orbitals in the wave functions increase as $\vec{k}$ moves away from $\vec{\Gamma}$ and is maximum at $\vec{R}$ in the Brillouin zone. The σ and σ^* bands are illustrated in Fig. 2.

D. σ nonbonding band

For the nearest-neighbor interaction model there is a flat nonbonding band denoted by σ^0. The wave functions consist entirely of $2p$ orbitals. The energy and wave-function amplitudes are given by

$$E_{\vec{k}\sigma^0}=E_\sigma, \tag{25}$$

$$c_\alpha^{\vec{k}\sigma^0}=\frac{S_\beta S_\gamma}{(S_x^2+S_y^2+S_z^2)^{1/2}}, \tag{26}$$

where α, β, or $\gamma=x$, y, or z with $\alpha\neq\beta\neq\gamma$.

If the oxygen-oxygen interactions are included, then first-order perturbation theory give the energy as

$$E_{\vec{k}\sigma^0}=\frac{E_\sigma-12[(pp\sigma)-(pp\pi)]S_x^2S_y^2S_z^2}{(S_x^2S_y^2+S_x^2S_z^2+S_y^2S_z^2)}. \tag{27}$$

The results of Eqs. (4)–(15) and (16)–(27) provide a complete analytical description of the 14 energy bands and the corresponding wave functions, from which all of the density functions can be computed. The energy bands of $KTaO_3$, shown in Fig. 2, are typical of those found for any of the cubic *d*-band perovskites.

III. DOS AND PDOS FUNCTIONS

A. Definitions

The DOS function $N^{\gamma}(E)$ for the γth energy band specifies the number of states in the energy interval between E and $E+dE$ *per unit cell* and is given by

$$N^{\gamma}(E)=2(a/\pi)^3\int d\vec{k}\,\delta(E-E_{\vec{k}\gamma})\ . \tag{28}$$

The integration is over the wave vectors in the first Brillouin zone,

$$\pi\geq 2k_{\alpha}a\geq -\pi;\ \ \alpha=x,\ y,\ \text{or}\ z\ ,$$

where $2a$ is the lattice parameter. The prefactor of 2 in Eq. (28) accounts for the two spin states.

Equation (28) may also be written as

$$N^{\gamma}(E)=\frac{-2}{\pi}(a/\pi)^3 \times \mathrm{Im}\left[\int d\vec{k}(E-E_{\vec{k}\gamma}+i0^{+})^{-1}\right]\ , \tag{29}$$

where 0^{+} is real, positive, and infinitesimal.

It is often convenient to work with a function of $E_{\vec{k}\gamma}$ rather than with $E_{\vec{k}\gamma}$ itself. Suppose that $g(E_{\vec{k}\gamma})$ is a single-valued function of $E_{\vec{k}\gamma}$ in some energy range. Then, in this energy range we have

$$\delta(E-E_{\vec{k}\gamma})=\left|\frac{\partial g(E)}{\partial E}\right|\delta(g(E)-g(E_{\vec{k}\gamma}))\ . \tag{30}$$

Thus,

$$N^{\gamma}(E)=2(a/\pi)^3\int d\vec{k}\left|\frac{\partial g(E)}{\partial E}\right|\delta(g(E)-g(E_{\vec{k}\gamma}))\ , \tag{31}$$

or

$$N^{\gamma}(E)=\frac{-2}{\pi}(a/\pi)^3\mathrm{Im}\left[\int d\vec{k}\left|\frac{\partial g(E)}{\partial E}\right|[g(E)-g(E_{\vec{k}\gamma})+i0^{+}]^{-1}\right]\ . \tag{32}$$

The PDOS function $P_{jq}^{\gamma}(E)$ for the γth band specifies the number of states in the energy interval between E and $E+dE$ *per unit cell* weighted by the square of the amplitude of the jqth orbital. That is, it is the spectral density of the jq-orbital component.

The PDOS is defined by

$$\begin{aligned}P_{jq}^{\gamma}(E)&=2(a/\pi)^3\int d\vec{k}\,|c_{jq}^{\vec{k}\gamma}|^2\delta(E-E_k)=\frac{-2}{\pi}(a/\pi)^3\mathrm{Im}\left[\int d\vec{k}\,|c_{jq}^{\vec{k}\gamma}|^2(E-E_{\vec{k}\gamma}+i0^{+})^{-1}\right]\\&=2(a/\pi)^3\int d\vec{k}\left|\frac{\partial g(E)}{\partial E}\right||c_{jq}^{\vec{k}\gamma}|^2\delta(g(E)-g(E_{\vec{k}\gamma}))\\&=\frac{-2}{\pi}(a/\pi)^3\mathrm{Im}\left[\int d\vec{k}\left|\frac{\partial g(E)}{\partial E}\right||c_{jq}^{\vec{k}\gamma}|^2[g(E)-g(E_{\vec{k}\gamma})+i0^{+}]^{-1}\right]\ .\end{aligned} \tag{33}$$

From Eq. (2b), it follows that

$$N^{\gamma}(E)=\sum_{jq}P_{jq}^{\gamma}(E)\ . \tag{34}$$

A large number of intermediate DOS and PDOS functions can be defined. For example, the total DOS functions associated with the various bands are given by

$$N_t^{\Gamma}(E)=\sum_{(\gamma=\Gamma\,\text{type})}N^{\gamma}(E)\ , \tag{35a}$$

$$P_p^{\Gamma}(E)=\sum_{(\gamma=\Gamma\,\text{type})}\ \sum_{(jq=\text{ox})}P_{jq}^{\gamma}(E)\ , \tag{35b}$$

$$P_d^{\Gamma}(E)=\sum_{(\gamma=\Gamma\,\text{type})}\ \sum_{(jq=d)}P_{jq}^{\gamma}(E)\ . \tag{35c}$$

In Eqs. (35a)–(35c) $\sum_{(\gamma=\Gamma\,\text{type})}$ indicates a sum

only over the Γ-type bands. The notation $\sum_{(jq=\mathrm{ox})}$ indicates a sum over the jq corresponding to oxygen-ion orbitals and $\sum_{(jq=d)}$ indicates a sum over the jq corresponding to the various d orbitals.

It is clear that the total DOS arising from all of the π bands, N^{π}, is given by

$$N^{\pi}(E)=N_t^{\pi}(E)+N_t^{\pi^*}(E)+N_t^{\pi^0}(E) . \tag{36}$$

Similarly, the total DOS associated with the σ bands, N^{σ}, is given by

$$N^{\sigma}(E)=N_t^{\sigma(+)}(E)+N_t^{\sigma(-)}(E)+N_t^{\sigma_0}(E) , \tag{37}$$

and the total DOS for all of the bands, both π and σ, is

$$N(E)=N^{\pi}(E)+N^{\sigma}(E) . \tag{38}$$

Similar definitions can be introduced for the PDOS functions and we shall introduce such functions as the need arises.

B. Van Hove singularities

In a subsequent section we shall see that the density-of-states functions have sharp features at special energies, called critical points. These sharp features, known as Van Hove singularities, arise from points in $\vec{k}$ space where the $\nabla_{\vec{k}} E_{\vec{k}} \mid_{\vec{k}=\vec{k}^0} = 0$. The nature of the Van Hove singularity depends upon the analytical character of the energy-band dispersion in the region of $\vec{k}$ space near $\vec{k}^0$, where the gradient of the energy vanishes. The classification of the singularities has been discussed in detail by Van Hove[21] and by Phillips.[22] We simply state some of the results here.

Let $E_0=E_{\vec{k}^0}$ be the energy at $\vec{k}^0$ for which the gradient vanishes. Near to E_0 the dispersion curve has an expansion of the form

$$E_{\vec{k}}=E_0+\sum_{i=1}^{L} a_i(k_i-k_i^0)^2 , \tag{39}$$

where k_i is the ith component of $\vec{k}$ in an orthogonal system of coordinates and $L=1$, 2, or 3 for one-, two-, or three-dimensional energy bands. For three-dimensional bands the singularities are labeled as M_0, M_1, M_2, M_3, where the subscript denotes the number of a_i's that are negative. The singularities are characterized as follows.

(i) M_0 point: The dispersion curve has a minimum at E^0. For $E>E_0$ and near E_0 the DOS function behaves as

$$\mathrm{const}(E-E_0)^{1/2},\ E \gtrsim E_0 \tag{40}$$

where const is a constant.

(ii) M_1 point: The dispersion curve has a (type I) saddle point at E_0. Near E_0 the DOS function behaves as

$$\begin{aligned} &\mathrm{const}-(E_0-E)^{1/2},\ E \lesssim E_0 \\ &\mathrm{const}-(E-E_0),\ E \gtrsim E_0 . \end{aligned} \tag{41}$$

(iii) M_2 point: The dispersion curve has a (type II) saddle point. Near E_0 the DOS functions behave as in Eq. (41) with E_0 and E interchanged.

(iv) M_3 point: The dispersion curve has a maximum at E_0. For E near to E_0 the DOS functions behave as

$$\mathrm{const}(E_0-E)^{1/2},\ E \lesssim E_0 . \tag{42}$$

The π bands of the perovskites are two dimensional[7] since, as can be seen from Eqs. (4) and (5), each of the energy bands depends only on two of the three components of the wave vector. For these bands the value of L appearing in Eq. (24) is 2. The Van Hove singularities of two-dimensional bands are denoted as P_0, P_1, and P_2, where again the subscript denotes the number of negative coefficients. The notation is given in what follows.

(v) P_0 point: The dispersion curve has a minimum at E_0. Near E_0 the DOS function has a jump discontinuiety of the form

$$\mathrm{const}\,\Theta(E-E_0),\ E \gtrsim E_0 \tag{43}$$

where $\Theta(x)=1$ for $x>0$ and 0 otherwise.

(vi) P_1 point: The dispersion curve has a saddle point. Near E_0 the DOS function has a logarithmic infinity of the form

$$\begin{aligned} &\mathrm{const}\ln(E_0-E),\ E<E_0 \\ &\mathrm{const}\ln(E-E_0),\ E>E_0 . \end{aligned} \tag{44}$$

(vii) P_2 points: The dispersion curve has a maximum at E_0. Near E_0 for $E<E_0$ the DOS function behaves as

$$\mathrm{const}\,\Theta(E_0-E)^{1/2} . \tag{45}$$

The PDOS function will display the same critical behavior as the DOS function unless the amplitude, $c_{qj}^{\vec{k}\nu}$ vanishes for $\vec{k}$ near $\vec{k}^0$.

C. Calculation of the PDOS and DOS for the π bands

The PDOS functions for the π bands are

$$P_{\alpha\beta}^{\gamma}(E)=2(a/\pi)^3 \int d\vec{k} \mid c_{\alpha\beta}^{\vec{k}\gamma} \mid^2 \delta(E-E_{\vec{k}\gamma}) , \tag{46}$$

$$P_\alpha^\gamma(E)=2(a/\pi)^3\int d\vec{k}\,|c_\alpha^{k\gamma}|^2\delta(E-E_{\vec{k}\gamma})\,,$$
$$\gamma=\pi(\alpha\beta)\text{ or }\pi(\alpha\beta)^*\,, \tag{47}$$

where $P_{\alpha\beta}^\gamma(E)$ is the PDOS for the $nd(\alpha\beta)$ orbital and $P_\alpha^\gamma(E)$ is the PDOS for the $2p(\alpha)$ orbital.

Referring to Eq. (7), we see that the nd-orbital amplitude is

$$|c_{\alpha\beta}^{\vec{k}\gamma}|^2=\frac{(E_{\vec{k}\gamma}-E_\pi)^2}{[(E_{\vec{k}\gamma}-E_\pi)^2+4(pd\pi)^2(S_\alpha^2+S_\beta^2)]}\,. \tag{48}$$

In the integrand of Eq. (46) we may place $|c_{\alpha\beta}^{\vec{k}\gamma}|^2$ by the value it takes on when the δ function is satisfied. From Eqs. (4) and (5) we see that we may make the replacements

$$E_{\vec{k}\gamma}\to E\,,$$
$$4(pd\pi)^2(S_\alpha^2+S_\beta^2)\to(E-E_t)(E-E_\pi)\,, \tag{49}$$

and obtain

$$P_{\alpha\beta}^\gamma(E)=\left|\frac{(E-E_\pi)}{2(E-E_{M\pi})}\right|2(a/\pi)^3\int dk\,\delta(E-E_{\vec{k}\gamma})$$
$$=\left|\frac{(E-E_\pi)}{(E-E_{M\pi})}\right|\rho_\pi^\gamma(E)\,, \tag{50}$$

where $E_{M\pi}=\frac{1}{2}(E_t+E_\pi)$ is the energy at the midgap between the π and π^* bands and we have introduced $\rho_\pi^\gamma(E)$ to represent the integral

$$(a/\pi)^3\int d\vec{k}\,\delta(E-E_{\vec{k}\gamma})\,. \tag{51}$$

Next we consider the PDOS functions for the $2p$ orbitals. It is useful to work with the sum of the $2p$-orbitals PDOS functions. In the case of the π bands the total $2p$ PDOS is

$$P_p^\gamma(E)=P_\alpha^\gamma(E)+P_\beta^\gamma(E)$$
$$=2(a/\pi)^3\int d\vec{k}\,(|c_\alpha^{\vec{k}\gamma}|^2+|c_\beta^{\vec{k}\gamma}|^2)$$
$$\times\delta(E-E_{\vec{k}\gamma})\,. \tag{52}$$

Using Eqs. (6) and making the replacements indicated in Eq. (49) gives the result that

$$P_p^\gamma(E)=2\left|\frac{(E-E_t)}{2(E-E_{M\pi})}\right|\rho_\pi^\gamma(E)\,. \tag{53}$$

Adding $P_p^\gamma(E)$ to $P_{\alpha\beta}^\gamma(E)$ gives, according to Eq. (28), the DOS function for the $\gamma=\pi(\alpha\beta)$ or $\gamma=\pi(\alpha\beta)^*$ band. It follows that

$$N^\gamma(E)=2\rho_\pi^\gamma(E)\quad[\gamma=\pi(\alpha\beta)\text{ or }\pi^*(\alpha\beta)]\,. \tag{54}$$

To find the PDOS and DOS functions we need to evaluate the integral $\rho_\pi^\gamma(E)$. To do this we define the dimensionless variable $\epsilon_\pi(E)$ by the relation

$$2+\epsilon_\pi(E)=\frac{[(E-E_{M\pi})^2-(\frac{1}{2}E_{g\pi})^2]}{2(pd\pi)^2}\,, \tag{55}$$

where $E_{g\pi}$ is the energy of the band gap between the π and π^* bands at Γ; $E_{g\pi}=E_t-E_\pi$. The energy-dispersion curves for the π bands may be written in a simplified form in terms of $\epsilon_\pi(E_{\vec{k}\gamma})$. The dispersion curves are given by:

$$\epsilon_\pi(E_{\vec{k}\gamma})=-(C_{2\alpha}+C_{2\beta})\,,$$
$$C_{2\alpha}=\cos(2k_\alpha a)\,. \tag{56}$$

According to Eq. (31) the integral $\rho_\pi^\gamma(E)$ can be written as

$$\rho_\pi^\gamma(E)=\left|\frac{(E-E_{M\pi})}{(pd\pi)^2}\right|(a/\pi)^3$$
$$\times\int d\vec{k}\,\delta(\epsilon_\pi+C_{2\alpha}+C_{2\beta})\,. \tag{57}$$

It should be noted that after performing the integration the right-hand side (rhs) of Eq. 57 is independent of the band index γ and thus both $\rho_\pi^{\pi(\alpha\beta)}$ and $\rho_\pi^{\pi(\alpha\beta)^*}$ are represented by the same function. In fact, the rhs of Eq. (57) represents $\rho_\pi^{\pi(\alpha\beta)}$ for $E<E_{M\pi}$ and $\rho_\pi^{\pi(\alpha\beta)^*}$ for $E>E_{M\pi}$. To be more precise we should write in place of Eq. (57) the equations

$$N^{\pi(\alpha\beta)}=\rho_\pi(E)\Theta(E_{M\pi}-E)\,,$$
$$N^{\pi(\alpha\beta)^*}=\rho_\pi(E)\Theta(E-E_{M\pi})\,, \tag{58}$$

where $\Theta(x)$ is the unit step function and $\rho_\pi(E)$ is equal to the rhs of Eq. (57) for all E. A superscript for the band index is not necessary for $\rho_\pi(E)$ and hence is omitted.

To evaluate $\rho_\pi(E)$ we perform the k_z integration and introduce the variables $t=C_{2\alpha}$ and $s=C_{2\beta}$. We then obtain the result

$$(a/\pi)^3\int dk_x\int dk_y\int dk_z\,\delta(\epsilon_\pi+C_{2\alpha}+C_{2\beta})$$
$$=\frac{1}{\pi^2}\int_{-1}^{1}ds\int_{-1}^{1}dt\frac{\delta(\epsilon_\pi+s+t)}{[(1-t^2)(1-s^2)]^{1/2}}$$
$$=\frac{1}{\pi^2}\int_{-1}^{1}\frac{dt\,\Theta(1-(\epsilon_\pi+t)^2)}{\{(1-t^2)[1-(\epsilon_\pi+t)^2]\}^{1/2}}\,. \tag{59}$$

It is seen from the rhs of Eq. (59) that the integral vanishes for $|\epsilon_\pi|>2$. For $|\epsilon_\pi|<2$ we may write

$$\rho_\pi(E)=\left|\frac{(E-E_{M\pi})}{\pi^2(pd\pi)^2}\right| \times\int_b^c \frac{dt}{[(a-t)(b-t)(t-c)(t-d)]^{1/2}}\ , \quad (60)$$

where $a\geq b\geq c\geq d$ with $a=1$, $b=1+\epsilon_\pi$, $c=-1$, and $d=\epsilon^\pi-1$ for $-2\leq\epsilon_\pi\leq 0$ and for $0\leq\epsilon_\pi\leq 2$, $a=1+\epsilon_\pi$, $b=1$, $c=\epsilon_\pi-1$, and $d=-1$. The integral in Eq. (60) is well known.[23] The final result is

$$\rho_\pi(E)=\left|\frac{(E-E_{M\pi})}{\pi^2(pd\pi)^2}\right|K(w)\Theta(w^2)\ , \quad w^2=1-(\epsilon_\pi/2)^2\ . \quad (61)$$

where K is the complete elliptic integral of the first kind,

$$K(x)=\int_0^{\pi/2}\frac{dt}{(1-x^2\sin^2 t)^{1/2}}\ . \quad (62)$$

Tabulations of $K(x)$ vs x are available.[23] The DOS functions are then given by the expressions

$$N^{\pi(\alpha\beta)}(E)=\left|\frac{2(E-E_{M\pi})}{\pi^2(pd\pi)^2}\right| \times K(w)\Theta(w^2)\Theta(E_{M\pi}-E)\ , \quad (63)$$

$$N^{\pi(\alpha\beta)^*}(E)=\left|\frac{2(E-E_{M\pi})}{\pi^2(pd\pi)^2}\right| \times K(w)\Theta(w^2)\Theta(E-E_{M\pi})\ . \quad (64)$$

For the PDOS functions we have

$$P^\gamma_{\alpha\beta}(E)=\left|\frac{(E-E_\pi)}{(E-E_{M\pi})}\right|N^\gamma(E)\ , \quad (65)$$

$$P^\gamma_\alpha(E)=\left|\frac{(E-E_t)}{(E-E_{M\pi})}\right|N^\gamma(E)\ , \quad (66)$$

$$\gamma=\pi(\alpha\beta)\text{ or }\pi(\alpha\beta)^*\ .$$

From Eqs. (4) and (5) it follows that the $\pi(\alpha\beta)$ band covers the range of energy,

$$E_\pi-W_\pi\leq E\leq E_\pi\ ,$$

while for the $\pi(\alpha\beta)^*$ band the range is

$$E_t\leq E\leq E_t+W_\pi\ ,$$

where

$$W_\pi=[(\tfrac{1}{2}E_{g\pi})^2+8(pd\pi)^2]^{1/2}\ .$$

It is easily verified that these two ranges correspond to $|\epsilon_\pi|\leq 2$ or $w^2\geq 0$. Hence, the density-of-states functions of Eqs. (63) and (64) vanish outside of the range of the π energy bands as, of course, they must.

It is worth noting that $N^{\pi(\alpha\beta)}(E)$ is the mirror reflection of $N^{\pi(\alpha\beta)^*}(E)$, about the line at $E=E_{M\pi}$; that is $\rho_\pi(E)$ is symmetric about $E=E_{M\pi}$. This feature is a direct consequence of the reflection symmetry of the conduction and valence π bands [Eqs. (4) and (5)].

There are three equivalent π (and π^*) bands corresponding to $\gamma=xy$, xz, and yz and also two possible spin states. Therefore the *total* DOS and PDOS functions are

$$N_t^\pi(E)=6\rho_\pi(E)\ , \quad (67)$$

$$P_d^\pi(E)=3\left|\frac{(E-E_\pi)}{(E-E_{M\pi})}\right|\rho_\pi(E)\ , \quad (68)$$

$$P_p^\pi(E)=3\left|\frac{(E-E_t)}{(E-E_{M\pi})}\right|\rho_\pi(E)\ . \quad (69)$$

The shapes of the functions N_t^π and P_d^π are illustrated in Figs. 3(a) and 3(b). It is clear that $N_t^\pi(E)$ possesses the P_0, P_1, and P_2 Van Hove singularities that are characteristic of two-dimensional bands. However, we also see that the P_2 peak is absent from P_d^π at E_π. This results because the *nd*-orbital amplitude vanishes at E_π. The function P_p^π is the reflection of P_d^π through the line $E_{M\pi}$ so that it vanishes at E_t. This is in accordance with the fact that the 2*p*-orbital amplitude vanishes at E_t. A comparison of $N(E)$ with the augmented-plane-wave (APW) results of Mattheiss[7] for $SrTiO_3$ is shown in Fig. 4. As can be seen, the agreement is excellent.

The values of the jump discontinuities are easily determined. The value of ϵ_π is ± 2 at the π or π^* band edges and hence at these points $w=0$. The value of $K(0)$ is $\frac{1}{2}\pi$ and hence the discontinuities are

$$\rho_\pi(E)\rightarrow\frac{E_{g\pi}}{4\pi(pd\pi)^2}\quad(E\rightarrow E_\pi\text{ or }E_t)\ , \quad (70)$$

$$N_t^\pi(E)\rightarrow\frac{3E_{g\pi}}{2\pi(pd\pi)^2}\quad(E\rightarrow E_\pi\text{ or }E_t)\ , \quad (71)$$

$$P_d^\pi(E)\rightarrow 0\quad(E\rightarrow E_\pi)\ , \quad (72a)$$

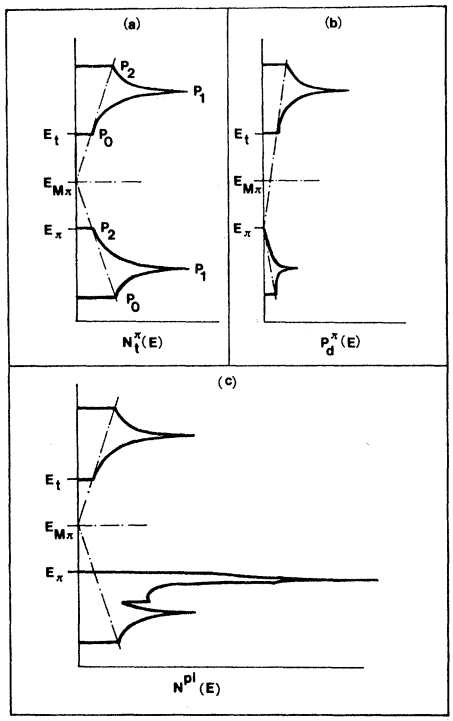

FIG. 3. Schematic illustrations of some of the density-of-states functions. (a) $N_t^\pi(E)$, (b) $P_d^\pi(E)$, and (c) the DOS function $N^\pi(E)$ including the contributions from the π, π^*, and π^0 bands. The structure and peak nearest to E_π arises from the π^0 nonbonding bands. The lowest-energy peak and lowest discontinuity comes from the π bands. Both the π and π^0 bands contribute to the discontinuity at E_π. The structure above $E_{M\pi}$ is due to the π^* bands.

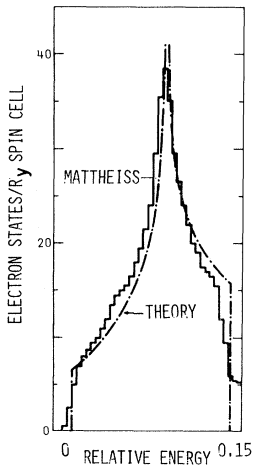

FIG. 4. Quantitative comparison of the total DOS associated with the π^* bands with the histogram of Mattheiss (Ref. 1) based on his augmented-plane-wave calculations for $SrTiO_3$. The parameters used in the theoretical calculation are $E_{g\pi}=3.25$ eV and $(pd\pi)=1.34$ eV.

$$P_d^\pi(E)\rightarrow\frac{3E_{g\pi}}{2\pi(pd\pi)^2}\quad(E\rightarrow E_t)\,, \tag{72b}$$

$$P_p^\pi(E)\rightarrow\frac{3E_{g\pi}}{2\pi(pd\pi)^2}\quad(E\rightarrow E_\pi)\,, \tag{72c}$$

$$P_p^\pi(E)\rightarrow 0\quad(E\rightarrow E_t)\,. \tag{72d}$$

From Eqs. (70)–(72) it can be seen that the height of the jump is proportional to the energy gap and inversely proportional to the square of the interaction parameter $(pd\pi)$. The energy gap $E_{g\pi}$ is a measure of the ionic character and $(pd\pi)$ is a measure of the covalent bonding between the transition-metal ion and oxygen ions. Thus, our results predict that the height of the jump will be largest for the most ionic perovskite.

The jump discontinuity in the DOS function can easily be seen in x-ray photoelectron spectroscopy (XPS) data that has been reported for $NaWO_3$ (Refs. 17 and 24). The joint density of states will also show a rapid increase associated with the band-edge behavior and such an effect can be seen in optical data for $SrTiO_3$ (Refs. 7 and 10).

D. Calculation of the DOS for the π nonbonding bands

For the nearest-neighbor interaction model the energy of the π^0 bands is constant, $E_{\vec{k}\pi^0}(\alpha\beta)=E_\pi$, and therefore the DOS function is just $\delta(E-E_\pi)$. Also, since the wave functions contain only oxygen $2p$ orbitals the PDOS function is the same as the DOS.

When the oxygen-oxygen ion interactions are included in the linear combinations of Löwdin orbitals (LCLO) model the π^0 bands have nonconstant energy as described in Sec. III B, Eq. (15). In this section we calculate the effect of this dispersion on the DOS function.

The calculation is facilitated by introducing the dimensionless variable $\epsilon_{\pi^0}(E)$, defined by

$$1+\epsilon_{\pi^0}(E)=\frac{\{E-E_\pi-[\frac{1}{2}b-(pp\pi)]\}}{[\frac{1}{2}b+(pp\pi)]}\,,$$
$$b=(pp\sigma)-(pp\pi)\,. \tag{73}$$

The π^0 energy is then given by

$$\epsilon_{\pi^0}(E_{\vec{k}\pi^0(\alpha\beta)})=-(C_{2\alpha}+C_{2\beta}+1)+\gamma C_{2\alpha}C_{2\beta}\,,$$
$$\gamma=\frac{\frac{1}{2}b-(pp\pi)}{\frac{1}{2}b+(pp\pi)}\,. \tag{74}$$

The bandwidth W_{π^0} of the π^0 band depends upon γ,

$$W=\begin{cases}2b, & |\gamma|\geq 1\\ 2[b+2(pp\pi)], & |\gamma|\leq 1\end{cases}. \tag{75}$$

For the perovskites $|(pp\sigma)|>|(pp\pi)|$ with $(pp\sigma)<0$ and $(pp\pi)>0$. Consequently, γ is usually greater than 1. For $SrTiO_3$ the value of γ ranges between 1.3 and 1.8 depending upon the calculational model. In what follows we shall assume that $\gamma>1$. The method employed in the calculations can, however, be used for any value of γ.

The DOS function is

$$N^{\pi^0(\alpha\beta)}(E)=2\left|\tfrac{1}{2}b+(pp\pi)\right|^{-1}\rho^{\pi^0(\alpha\beta)}(\epsilon_{\pi^0}),$$
$$\rho^{\pi^0(\alpha\beta)}(\epsilon_{\pi^0})=\int d\vec{k}\,\delta(\epsilon_{\pi^0}-\epsilon_{\pi^0}(E_{\vec{k}\,\pi^0(\alpha\beta)})). \tag{76}$$

The DOS is obviously independent of $\alpha\beta$ and therefore to simplify the notation we shall omit the $(\alpha\beta)$ descriptor whenever possible. Using Eqs. (73) and (76) we obtain

$$\rho^{\pi^0}(\epsilon_{\pi^0})=\frac{1}{\pi^2}\int_0^{\pi}\frac{dx}{(\gamma C_x-1)}\int_0^{\pi}dy\,\delta\left[\left[\frac{\epsilon_{\pi^0}+C_x+1}{\gamma C_x-1}\right]-C_y\right]$$
$$=\frac{1}{\pi^2}\int_{-1}^{1}dr\,\frac{\Theta\left[1-\left[\dfrac{1+\epsilon_{\pi^0}+r}{\gamma r-1}\right]^2\right]}{(1-r^2)^{1/2}[(\gamma r-1)^2-(\epsilon_{\pi^0}+r+1)^2]^{1/2}}. \tag{77}$$

It is easily verified that the Θ function in the integrand of Eq. (77) vanishes for E outside of the π^0 energy-band range; that is, for $|\epsilon_{\pi^0}|>1+\gamma$. The Θ function also has the effect of limiting the integration on r to ranges of r for which the factors in the square root are both positive. The evaluation of the integral in Eq. (77) is straightforward but tedious. The results are

$$\rho^{\pi^0}(\epsilon_{\pi^0})=\frac{2n}{\pi^2[(\gamma^2-1)(a-c)(b-d)]^{1/2}}K\left[\left[\frac{(a-b)(c-d)}{(a-c)(b-d)}\right]^{1/2}\right]\Theta((1+\gamma)^2-\epsilon_{\pi^0}^2), \tag{78}$$

The constants n, a, b, c, and d depend on the range of ϵ_{π^0}.

For $-(1+\gamma)\leq\epsilon_{\pi^0}\leq-(1+\gamma)/\gamma$:

$n=2$,

$a=1$,

$b=-\epsilon_{\pi^0}/(1+\gamma)$,

$c=(2+\epsilon_{\pi^0})/(\gamma-1)$,

$d=-1$.

For $-(1+\gamma)/\gamma\leq\epsilon_{\pi^0}\leq(\gamma-3)$:

$n=2$,

$a=1$,

$b=(2+\epsilon_{\pi^0})/(\gamma-1)$,

$c=-\epsilon_{\pi^0}/(1+\gamma)$,

$d=-1$.

For $(\gamma-3)\leq\epsilon_{\pi^0}\leq(1+\gamma)$:

$n=1$,

$a=(2+\epsilon_{\pi^0})/(\gamma-1)$,

$b=1$,

$c=-\epsilon_{\pi^0}/(\gamma+1)$,

$d=-1$.

A schematic of ρ^{π^0} vs ϵ_{π^0} is shown in Fig. 5. The functions have jump discontinuities at $\epsilon_{\pi^0}=-(1+\gamma)$, $(\gamma-3)$, and $(\gamma+1)$ and a logarithmic singularity at $\epsilon_{\pi^0}=-(1+\gamma)/\gamma$. The magnitudes of the jump discontinuities are given in the caption of Fig. 5. Since there are three equivalent π^0 bands the total π^0 DOS (including a factor of 2 for the spin states) is

$$N_t^{\pi^0}(E)=6\rho^{\pi^0}(E). \tag{79}$$

E. Total DOS for all π bands

The total DOS function for the π, π^0, and π^* bands is just the sum of the corresponding DOS

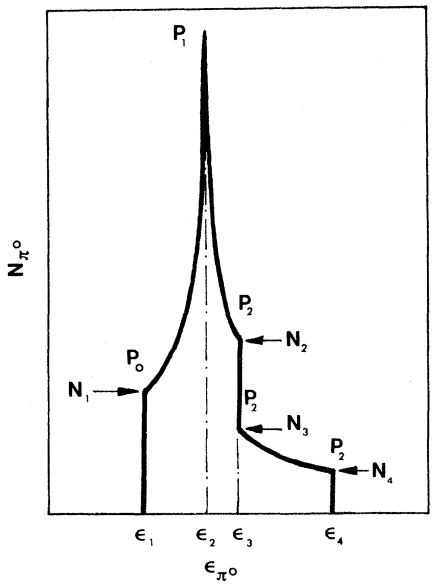

FIG. 5. Schemtatic illustration of the function $N^{\pi^0}(E)$. The jump discontinuity at $\epsilon_1=-(1+\gamma)$ is $N_1=(\gamma^2-1)^{-1/2}$. At $\epsilon_2=-(1+\gamma)/\gamma$ there is a P_1 logarithmic infinity. At $\epsilon_3=(\gamma-3)$, $N_2=(\gamma-1)^{-1}$, and $N_3=\frac{1}{2}N_2$. At $\epsilon_4=(1+\gamma)$, $N_4=\frac{1}{2}(\gamma+1)^{-1}$.

functions. Thus the DOS function for all the π bands, $N^{\pi}(E)$ is

$$N^{\pi}(E)=N_t^{\pi}(E)+N_t^{\pi^0}(E) . \tag{80}$$

The total valence-bands DOS and conduction-band DOS functions are given by

$$[N^{\pi}(E)]_v=N^{\pi}(E)\Theta(E_{M\pi}-E) , \tag{81a}$$

$$[N^{\pi}(E)]_c=N^{\pi}(E)\Theta(E-E_{M\pi}) , \tag{81b}$$

where v and c denote valence and conduction bands, respectively. A schematic of the function $N^{\pi}(E)$ is shown in Fig. 3(c). We have that

$$\int dE\, N^{\pi}(E)=18 , \tag{82a}$$

$$\int dE\, [N^{\pi}(E)]_v=12 , \tag{82b}$$

$$\int dE\, [N^{\pi}(E)]_c=6 . \tag{82c}$$

Figure 4 shows a comparison of $[N^{\pi}(E)]_c$ with the numerical results of Mattheiss[1] (based on an augmented-plane-wave calculation) for $SrTiO_3$. The quantitative agreement is seen to be excellent. Similar agreement is found between $[N^{\pi}(E)]_c$ and XPS data for $NaWO_3$ (Ref. 17).

F. DOS for the σ and σ^* bands

In this section we investigate the DOS functions for the σ and σ^* bands. Because of the complexity of the energy-band dispersion [Eqs. (6) and (7)] it is not possible to obtain exact results for the DOS functions. Fortunately, however, very simple and highly accurate approximations can be obtained.

We begin with a discussion of the symmetry properties of the $\sigma(\pm)$ and $\sigma^*(\pm)$ bands and show that a knowledge of the DOS for any one of these four bands is sufficient to determine all of the DOS functions. Next, we determine the behavior of the DOS functions at each of the critical points. The critical-point information is then used to construct approximate DOS functions which accurately represent the exact functions.

G. Symmetry properties of the σ and σ^* bands

Using Eqs. (6) and (7) we find that the energy-band dispersion curves for the $\sigma(\pm)$ and $\sigma^*(\pm)$ bands satisfy the relation

$$\begin{aligned}&(E_e-E_{\vec{k}\nu(\eta)})(E_\sigma-E_{\vec{k}\nu(\eta)})\\&\quad=2(pd\sigma)^2(S_x^2+S_y^2+S_z^2+\eta S^2) ,\\&\eta=+\text{ or }-,\ \nu=\sigma\text{ or }\sigma^* .\end{aligned} \tag{83}$$

It is convenient to introduce the dimensionless variable $\epsilon_\sigma(E)$ defined by

$$\epsilon_\sigma(E)=(E_e-E)(E_\sigma-E)/(pd\sigma)^2-3 . \tag{84}$$

The energy-band relation of Eq. (83) may then be expressed as

$$\begin{aligned}&\epsilon_\sigma(E_{\vec{k}\nu(\eta)})=-(C_{2x}+C_{2y}+C_{2z})+\eta C ,\\&C_{2\alpha}=\cos(2\vec{k}_\alpha a) ,\\&C=(C_{2x}^2+C_{2y}^2+C_{2z}^2-C_{2x}C_{2y}\\&\qquad-C_{2x}C_{2z}-C_{2y}C_{2z})^{1/2} .\end{aligned} \tag{85}$$

It is easily verified that

$$\epsilon_\sigma(E_{\vec{k}\sigma(\eta)})=\epsilon_\sigma(E_{\vec{k}\sigma^*(\eta)}) \tag{86}$$

for every choice of the vector $\vec{k}$. The function ϵ_σ maps both the $\sigma(\eta)$ and $\sigma^*(\eta)$ bands into a common curve. This is possible becase $E_{\vec{k}\sigma^*(\eta)}$ is the reflection of $E_{\vec{k}\sigma(\eta)}$ through the line at the middle of the gap between the σ and σ^* bands at $E_{M\sigma}=\frac{1}{2}(E_e+E_\sigma)$. As a consequence of this mapping it is clear that the DOS, as a function of ϵ_σ, will be

the same for both the $\sigma(\eta)$ and $\sigma^*(\eta)$ bands.

In order to simplify the notation we shall henceforth denote $\epsilon_\sigma(E_{\vec{k}\nu(\eta)})$ by simply $\epsilon_{\vec{k}\nu(\eta)}$, with $\eta=+$ or $-$ and $\nu=\sigma$ or σ^*. The two branches, corresponding to $\eta=+$ and $-$, are shown in Fig. 2.

We define the function $\rho^{\nu(\eta)}(\epsilon_\sigma)$ by

$$\rho^{\nu(\eta)}=(a/\pi)^3\int d\vec{k}\,(\epsilon_\sigma-\epsilon_{\vec{k}\nu(\eta)}) =\frac{-1}{\pi}\mathrm{Im}\left[(a/\pi)^3\int d\vec{k}\,(\epsilon_\sigma-\epsilon_{\vec{k}\nu(\eta)}+i0^+)^{-1}\right], \quad (87)$$

where $2a$ is the lattice parameter, the integration is over the first Brillouin zone, and 0^+ is a positive infinitesimal. According to Eq. (31), the desired DOS functions in E space, $N^{\nu(\eta)}$, can be obtained from $\rho^{\nu(\eta)}$ through the relations

$$N^{\nu(\eta)}(E)=2\left|\frac{d\epsilon_\sigma(E)}{dE}\right|\rho^{\nu(\eta)}(\epsilon_\sigma(E)) =\left[\frac{|E_{M\sigma}-E|}{(pd\sigma)^2}\right]\rho^{\nu(\eta)}(\epsilon_\sigma(E)) . \quad (88)$$

The relationship expressed by Eq. (88) represents $N^{\sigma(\eta)}$ for $E\le E_{M\sigma}$ and $N^{\sigma^*(\eta)}$ for $E>E_{M\sigma}$. The precise statement is

$$N^{\sigma(\eta)}(E)=\left[\frac{|E_{M\sigma}-E|}{2(pd\sigma)^2}\right] \times 2\rho^{\sigma(\eta)}(\epsilon_\sigma(E))\Theta(E_{M\sigma}-E) , \quad (89)$$

$$N^{\sigma^*(\eta)}(E)=\left[\frac{|E_{M\sigma}-E|}{2(pd\sigma)^2}\right] \times 2\rho^{\sigma^*(\eta)}(\epsilon_\sigma(E))\Theta(E-E_{M\sigma}) , \quad (90)$$

where $\Theta(x)$ is the unit step function; $\Theta(x)=1$ for $x>0$ and 0 otherwise.

There is a simple relationship between the two branches expressed by

$$\epsilon_{\vec{k}\nu(+)}=-\epsilon_{\vec{k}'\nu(-)},\quad \vec{k}'=\vec{k}-\vec{R} \quad (91)$$

where $\vec{R}$ is the vector $(2a/\pi)(1,1,1)$. Equation (91) states that the $(+)$ branch may be converted to the $(-)$ branch by adding the vector $\vec{R}$ to the $\vec{k}$ vector and then inverting the resulting curve. From this relation it follows that

$$\rho^{\nu(+)}(\epsilon_\sigma)=\rho^{\nu(-)}(-\epsilon_\sigma),\quad \nu=\sigma \text{ or } \sigma^* . \quad (92)$$

Therefore, if one of the DOS functions is known then the other is also known. The total density, $\rho^\sigma(\epsilon_\sigma)$, including both the plus and minus branches, will be given by

$$\rho^\sigma(\epsilon_\sigma)=\rho^{\sigma(+)}(\epsilon_\sigma)+\rho^{\sigma(-)}(\epsilon_\sigma) =\rho^{\sigma(-)}(\epsilon_\sigma)+\rho^{\sigma(-)}(-\epsilon_\sigma) . \quad (93)$$

Equation (93) makes it obvious that $\rho^\sigma(\epsilon_\sigma)$ must be symmetric about $\epsilon_\sigma=0$. In summary, we have shown that the total DOS function can be obtained from a knowledge of either $\rho^{\sigma(+)}(\epsilon_\sigma)$ or $\rho^{\sigma(-)}(\epsilon_\sigma)$.

H. Analytical behavior of the σ DOS function

Our next task in determining the DOS function is to find the behavior of the function near the critical points. The critical energies will be associated with the regions of $\vec{k}$ space where the gradient of the energy vanishes; that is where $\nabla_{\vec{k}}E_{\vec{k}\sigma(\eta)}=0$.

A simple calculation using Eq. (85) shows that the critical energies are those attained when the $\vec{k}$ vector is near the $\overline{\Gamma X}$ or $\overline{MR}$ lines, or the M, X, or R points in the Brillouin zone. The critical energies correspond to the values of $\epsilon_{\vec{k}\sigma(-)}$ given below:

$$\begin{aligned}&(a)\ -3;\ \vec{k} \text{ near the } \overline{\Gamma X} \text{ lines},\\ &(b)\ -1;\ \vec{k} \text{ near the } \vec{M} \text{ points},\\ &(c)\ +3;\ \vec{k} \text{ near the } \vec{R} \text{ points} .\end{aligned} \quad (94)$$

For $\epsilon_{\vec{k}\sigma}(+)$ the critical energies correspond to

$$\begin{aligned}&(a')\ 3;\ \vec{k} \text{ near the } \overline{MR} \text{ lines},\\ &(b')\ -3;\ \vec{k} \text{ near the } \vec{X} \text{ points},\\ &(c')\ -3;\ \vec{k} \text{ near the } \vec{\Gamma} \text{ points} .\end{aligned} \quad (95)$$

From the symmetry arguments presented previously it follows that the analytic behavior of $\epsilon_{\vec{k}\sigma(-)}$ near the critical points (a), (b), and (c) of Eq. (94) is the same as that of $\epsilon_{\vec{k}\sigma(+)}$ at (a'), (b'), and (c') of Eq. (95), respectively.

We begin our analysis by slowing the $\rho^{\sigma(-)}$ has a P_0 critical behavior near $\epsilon_{\vec{k}\sigma(-)}=-3$ due to the contributions form $\vec{k}$ space near a $\overline{\Gamma X}$ line. The P_0 critical behavior is a jump discontinuity, characteristic of an energy-dispersion curve which

has a two-dimensional nature. If we consider a cylinder in $\vec{k}$ space whose axis is a $\overline{\Gamma X}$ line and whose radius r_0 is very small, then $\epsilon_{\vec{k}\sigma(-)}$ has the quadratic expansion

$$\epsilon_{\vec{k}\sigma(-)}=-3+(\tfrac{3}{4})r^2 , \tag{96}$$

where $r^2=(2\vec{k}_\alpha a)^2+(2\vec{k}_\beta a)^2$. The limiting form of the DOS for $\rho^{\sigma(-)}$ as $\epsilon_\sigma\to -3+0^+$ is

$$\lim_{\epsilon_\sigma\to -3+0^+}[\rho^{\sigma(-)}(\epsilon_\sigma)]=\frac{-1}{\pi}\mathrm{Im}\left[1/(2\pi)^2\int_0^{2\pi}d\phi\int_0^{r_0}r\,dr[(\epsilon_\sigma+3)-\tfrac{3}{4}r^2+i0^+]^{-1}\right]$$
$$=\frac{1}{3\pi}\Theta(\epsilon_\sigma+3) . \tag{97}$$

We see from Eq. (97) that there is a jump discontinuity in $\rho^{\sigma(-)}$ of the magnitude of $1/3\pi$ due to the flat dispersion curve along the $\overline{\Gamma X}$ line. Since there are three equivalent $\overline{\Gamma X}$ lines in the Brillouin zone the total discontinuity will be $1/\pi$. Also, from symmetry considerations it must be that $\rho^{\sigma(+)}$ has the same jump as $\epsilon_\sigma\to 3-0^+$.

Now let us consider the behavior of $\rho^{\sigma(+)}(\epsilon_\sigma)$ near $\epsilon_\sigma=-3+0^+$, which occurs for $\vec{k}$ vectors near to Γ. We have the expansion

$$\epsilon_{\vec{k}\sigma(+)}=-3+2\xi^2+2[\xi^4-3(x^2y^2+x^2z^2+y^2z^2)]^{1/2} , \tag{98}$$

where $x=k_x a$, $y=k_y z$, $z=k_z a$, and $\xi^2=x^2+y^2+z^2$. In spherical coordinates we have

$$\epsilon_{k\sigma(+)}=-3+2\xi^2 f(\theta,\phi) ,$$
$$f(\theta,\phi)=1+[1-3\sin^2\theta(\sin^2\phi\cos^2\phi\sin^2\phi+\cos^2\phi)]^{1/2} , \tag{99}$$

where in Eq. (98) we have made the substitution $x=\xi\sin\cos\phi$, $y=\sin\xi\sin\theta$, and $z=\xi\cos\theta$.

The energy expression of Eq. (98) is quadratic in the three components of the wave vector $\vec{k}$ and the coefficients ($f(\theta,\phi)$) are all positive. Therefore as described previously the crtical behavior is that of an M_0 point and the behavior of the DOS is

$$\rho^{\sigma(+)}(\epsilon_\sigma)\to\mathrm{const}(\epsilon_\sigma+3)^{1/2} . \tag{100}$$

From symmetry considerations it follows that $\rho^{\sigma(-)}$ has the M_3 behavior for ϵ_σ near to 3,

$$\rho^{\sigma(-)}(\epsilon_\sigma)\to\mathrm{const}(3-\epsilon_\sigma)^{1/2} . \tag{101}$$

The dispersion curves for $\epsilon_{\vec{k}\sigma(+)}$ and $\epsilon_{\vec{k}\sigma(-)}$ have saddle points near $\epsilon_\sigma=1$ and $\epsilon_\sigma=-1$, respectively. This may be seen considering the behavior of $\epsilon_{\vec{k}\sigma(-)}$ for $\vec{k}$ vectors in a small sphere centered on an X point in the Brillouin zone. One has that

$$\epsilon_{\vec{k}\sigma(+)}=1-(\pi-2\vec{k}_\alpha a)^2+(\vec{k}_\beta a)^2+(\vec{k}_\gamma a)^2 . \tag{102}$$

The quadratic form contains one negative coefficient and as described previously the DOS function will have an M_1 critical behavior,

$$\rho^{\sigma(+)}(\epsilon_\sigma)\to\begin{cases}\mathrm{const}-(1-\epsilon_\sigma)^{1/2}\text{ as }\epsilon_\sigma\to 1-0^+\\ \mathrm{const}-(\epsilon_\sigma-1)\text{ as }\epsilon_\sigma\to 1+0^+ .\end{cases} \tag{103}$$

Then from symmetry considerations it follows that $\rho^{\sigma(-)}$ must have an M_2-type behavior for ϵ_σ near -1 of the form:

$$\rho^{\sigma(-)}(\epsilon_\sigma)\to\begin{cases}\mathrm{const}+(1+\epsilon_\sigma)\text{ as }\epsilon_\sigma\to -1-0^+\\ \mathrm{const}-(1+\epsilon_\sigma)^{1/2}\text{ as }\epsilon_\sigma\to -1+0^+ .\end{cases} \tag{104}$$

Using the results derived above the qualitative behavior of the DOS functions $\rho^{\sigma(-)}$, $\rho^{\sigma(+)}$, and ρ^σ can be understood. Figure 6 shows graphs of these functions obtained by numerical calculations.

I. Analytical formulas for the DOS of the σ and σ^* bands

From the results of the preceding section we know the analytical behavior of $\rho^{\sigma(-)}$ near the critical energies. Using this information we have developed an analytical approximation for $\rho^{\sigma(-)}$ which differs from

the exact function (calculated numerically) by less than 3% for any value of ϵ_σ. The approximate function is

$$\pi\rho^{\sigma(-)}(\epsilon_\sigma)=\begin{cases}1+\alpha x^2+\frac{1}{2}\mathrm{sgn}(\epsilon_\sigma)\left[1-\frac{1}{\pi}\sqrt{x(1-x)}-\frac{1}{2}\sqrt{x(3-2x)}\right], & 1\le|\epsilon_\sigma|\le 2\\ \frac{1}{2}(1+\alpha)-\frac{1}{4}(1-\epsilon_\sigma^2)^{1/2}+\frac{1}{\pi}\left[1-\frac{1}{2\pi}\right]\sin^{-1}(\epsilon_\sigma), & |\epsilon_\sigma|\le 1\\ 0, & |\epsilon_\sigma|>2\end{cases} \tag{105}$$

with $x=\frac{1}{2}(3-|\epsilon_\sigma|)$ and $\alpha=\frac{1}{2}(1-1/\pi)$. This function possesses the correct analytical behavior near the critical energies and satisfies the normalization condition that

$$\int_{-2}^{2}\rho^{\sigma(-)}(\epsilon_\sigma)d\epsilon_\sigma=1\ . \tag{106}$$

The total DOS for the σ or σ^* band, including a factor of 2 for spin states,

$$n^{\sigma^*}(E)=2\rho_\sigma(E)\Theta(E-E_{M\sigma})\ , \tag{107a}$$

$$n^{\sigma}(E)=2\rho_\sigma(E)\Theta(E_{M\sigma}-E)\ , \tag{107b}$$

$$N_t^\sigma(E)=n^{\sigma^*}(E)+n^\sigma(E)=2\rho_\sigma(E)\ , \tag{108}$$

$$\rho_\sigma(E)=\left[\frac{|E_{M\sigma}-E|}{2(pd\sigma)^2}\right]\times[\rho^{\sigma(-)}(\epsilon_\sigma(E))+\rho^{\sigma(-)}(-\epsilon_\rho(E))]\ . \tag{109}$$

The normalization conditions are

$$\int_{-\infty}^{\infty}\rho_\sigma(E)dE=\int_{E_e}^{\infty}n^{\sigma^*}(E)dE=\int_{-\infty}^{E_\sigma}n^\sigma(E)dE=4\ , \tag{110}$$

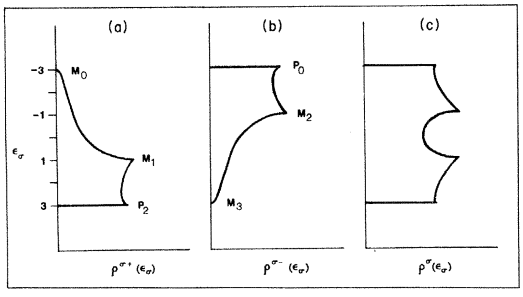

FIG. 6. Numerical calculation of the DOS; (a) $\rho^{\sigma(+)}$, (b) $\rho^{\sigma(-)}$, and (c) ρ^σ.

$$\int_{-\infty}^{\infty}N_t^\sigma(E)dE=8\ . \tag{111}$$

Equation (110) shows that there are four electronic states per unit cell for either the σ or σ^* bands. The function $N^{\sigma^*}(E)$ corresponds to the curve above E_e in Fig. 7(c).

J. Analytic formulas for the DOS of the σ^0 band

For the nonbonding σ^0 band we shall use the energy dispersion given by Eq. (27), which includes the effects of the oxygen-oxygen interactions. We neglect the very small mixing of the cation d orbitals into the nonbonding band wave functions. Thus the wave functions are assumed to be those whose amplitudes are specified by Eq. (26).

The dispersion curve specified by Eq. (27) can be expressed in terms of the dimensionless variable $\epsilon_0(E)$ defined by:

$$\epsilon_0(E)=(E_\sigma-E)/2b-1\qquad b=(pp\sigma)-(pp\pi)\ . \tag{112}$$

With this variable the energy dispersion may be expressed by:

$$\epsilon_0(E_{\vec{k}\sigma^0})=\frac{6S_x^2S_y^2S_z^2}{(S_x^2S_y^2+S_x^2S_z^2+S_y^2S_z^2)}-1\ . \tag{113}$$

The function $\rho^\sigma(\epsilon_\sigma)$ is

$$\rho^{\sigma^0}(\epsilon_\sigma)=(a/\pi)^3\int d\vec{k}\,\delta(\epsilon_0-\epsilon_0(E_{\vec{k}\sigma^0}))\ . \tag{114}$$

It is easily shown that the critical energies correspond to $\epsilon_0=-1$ and 1. The behavior of the DOS for $\epsilon_0\to 1$, arising from the region in $\vec{k}$ space near $\vec{\Gamma}$ is

$$\rho^{\sigma^0}(\epsilon_0)\rightarrow \text{const}(1+\epsilon_0)^{1/2} \text{ as } \epsilon_0\rightarrow -1+0^+ . \quad (115)$$

The region in $\vec{k}$ space near the $\vec{R}$ point produces a square-root singularity (characteristic of a one-dimensional dispersion relation) which is of the form:

$$\rho^{\sigma^0}(\epsilon_0)\rightarrow \text{const}(1-\epsilon_0)^{-1/2} \text{ as } \epsilon_\sigma\rightarrow 1-0^+ . \quad (116)$$

The DOS vanishes for $|\epsilon_\sigma|>1$.

An approximation for $\rho^{\sigma^0}(\epsilon_0)$ which deviates from the numerically calculated function by less than 5% at any point is

$$\rho^{\sigma^0}(\epsilon_0)=(\tfrac{5}{3}+\pi/2)^{-1}\left[(-\epsilon_0)+\frac{\Theta(\epsilon_0)}{\sqrt{1-\epsilon_0}}\right]$$

$$\times\sqrt{1+\epsilon_0}\Theta(1-\epsilon_0^2) . \quad (117)$$

The function of Eq. (117) gives the correct analytical behavior as $\epsilon_0\rightarrow -1$ or $+1$ and is normalized so that

$$\int_{-1}^{1}\rho^{\sigma^0}(\epsilon_0)d\epsilon_0=1 . \quad (118)$$

The DOS in E space, $N^{\sigma^0}(E)$, including a factor of 2 for the spin states, is given by

$$2\rho^{\sigma^0}(E)=N^{\sigma^0}(E)=2(1/|b|)\rho^{\sigma^0}(\epsilon_0(E)) \quad (119)$$

and the normalization is

$$\int_{E_\sigma-12b}^{E_\sigma}N^{\sigma^0}(E)dE=2 . \quad (120)$$

We shall refer to the total DOS for all of the σ band (σ, σ^*, and σ^0), as $N^\sigma(E)$. This function can be written as a sum of a valence-band and conduction-band total density,

$$N^\sigma(E)=[N^\sigma(E)]_v+[N^\sigma(E)]_c , \quad (121)$$

where

$$[N^\sigma(E)]_v=n^\sigma(E)+N^{\sigma^0}(E), \quad E\le E_\sigma \quad (122)$$

$$[N^\sigma(E)]_c=n^{\sigma^*}(E), \quad E\ge E_e . \quad (123)$$

We also have the normalizations

$$\int_{-\infty}^{E_\sigma}[N^\sigma(E)]_v dE=6 , \quad (124)$$

$$\int_{E_e}^{\infty}[N^\sigma(E)]_c dE=4 . \quad (125)$$

These functions are shown in Fig. 7(c). The curve above E_e is $[N^\sigma(E)]_c$ and the curve below E_σ is $[N^\sigma(E)\}_v$.

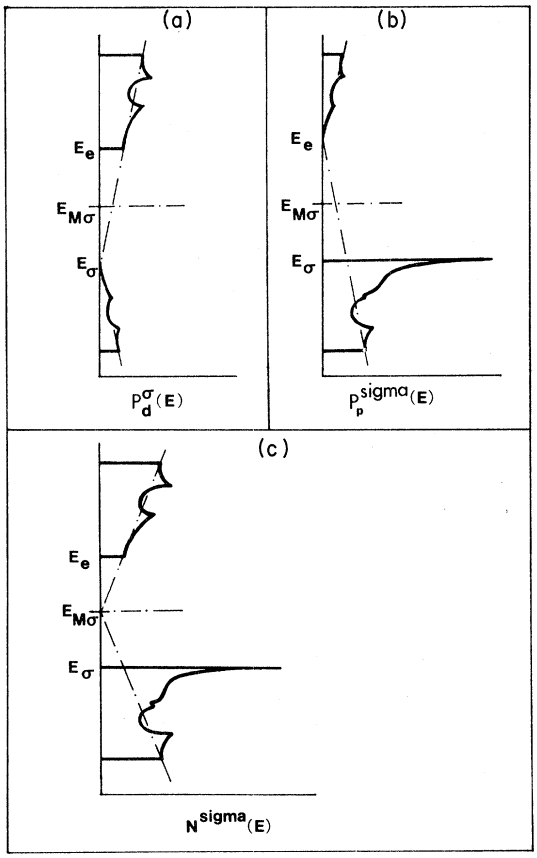

FIG. 7. PDOS functions; (a) shows the p-orbital PDOS, (b) shows the d-orbital PDOS, and (c) shows the total DOS for the σ bands.

K. Partial-density-of-states functions for the σ bands

In this section we discuss the PDOS functions associated with the σ bands. The PDOS functions give the number of electronic states per unit cell in the energy range dE and E associated with a particular type of orbital. For the perovskites we need to determine the PDOS functions assoicated with the e_g type of d orbitals of the B ions and the PDOS for the oxygen $2p$ orbitals which have a σ type of overlap with the e_g orbitals.

The PDOS functions are given by the expression

$$P_{qj}^{\nu}(E)=(a/\pi)^3\int dk\,|c_{qj}^{k\nu}|^2(E-E_{k\nu}) , \quad (126)$$

where $P_{qj}^{\nu}(E)$ is the PDOS function for the q-type symmetry orbitals on the jth ion for the band whose index is ν.

For the σ bands the total d-orbital PDOS, the sum of the PDOS functions for the $d(3z^2-r^2)$ and $d(x^2-y^2)$ orbitals summed over the four bands, is

$$P_d^\sigma(E)=\sum_{\nu\eta} P_d^{\nu\eta}(E)=2\sum_{\nu\eta}(a/\pi)^3\int dk(\,|\,c_{z^2}^{k\nu(\eta)}\,|^2+|\,c_{x^2}^{k\nu(\eta)}\,|^2)\delta(E-E_{k\nu(\eta)})\,, \tag{127}$$

where the factor of 2 accounts for the spin states and in Eq. (57); $\nu=\sigma$ or σ^* and $\eta=+$ or $-$.

The total $2p$-orbital PDOS, including the three oxygen ions per unit cell and the four bands is

$$P_p^\sigma(E)=2(a/\pi)^3\sum_{\nu\eta}\int dk(\,|\,c_x^{k\nu(\eta)}\,|^2+|\,c_y^{k\nu(\eta)}\,|^2+|\,c_z^{k\nu(\eta)}\,|^2)\delta(E-E_{k\nu(\eta)})\,. \tag{128}$$

The PDOS functions given by Eqs. (127) and (128) may be expressed directly in terms of the DOS functions for the σ bands. We make use of Eqs. (16) through (24) and the fact that the orbital amplitudes in the integrands of Eqs. (127) and (128) can be replaced by their values at $E_{k\nu(\eta)}=E$. After a considerable amount of algebra one finds that

$$P_d^\sigma(E)=\left|\frac{(E-E_\sigma)}{\frac{1}{2}(E-E_{M\sigma})}\right|[n^{\sigma^*}(E)+n^\sigma(E)]=2\left|\frac{(E-E_\sigma)}{(pd_\sigma)^2}\right|[\rho^{\sigma(-)}(\epsilon_\sigma(E))+\rho^{\sigma(-)}(-\epsilon_\sigma(E))]\,. \tag{129}$$

A similar calculation gives

$$P_p^\sigma(E)=\left|\frac{(E-E_e)}{\frac{1}{2}(E-E_{M\sigma})}\right|[n^{\sigma^*}(E)+n^\sigma(E)]=2\left|\frac{(E-E_e)}{(pd\sigma)^2}\right|[\rho^{\sigma(-)}(\epsilon_\sigma(E))+\rho^{\sigma(-)}(-\epsilon_\sigma(E))]\,. \tag{130}$$

The factors $|E-E_\sigma|$ in P_d^σ and $|E-E_e|$ in P_p^σ reflect the fact that the states are pure p or d orbitals, respectively, at the top of valence bands and at the botton of the conduction bands.

The PDOS functions satisfy the normalization conditions,

$$\int_{-\infty}^{\infty} P_d^\sigma(E)dE=\int_{-\infty}^{\infty} P_p^\sigma(E)dE=4\,. \tag{131}$$

The σ^0 nonbonding band has wave functions that are composed entirely of the oxygen $2p$ orbitals and hence,

$$\begin{aligned} P_p^{\sigma^0}(E)&=N^{\sigma^0}(E)\,,\\ P_d^{\sigma^0}(E)&=0\,. \end{aligned} \tag{132}$$

The total PDOS functions, including the σ, σ^* and σ^0 band and spin are,

$$\begin{aligned} P_d^\sigma(E)&=P_d^\sigma(E)\,,\\ P_p^\sigma(E)&=P_p^\sigma(E)+N^{\sigma^0}(E)\,, \end{aligned} \tag{133}$$

and

$$\begin{aligned} \int_{-\infty}^{\infty} P_d^\sigma(E)dE&=4\,,\\ \int_{-\infty}^{\infty} P_p^\sigma(E)dE&=6\,. \end{aligned} \tag{134}$$

The functions P_p^σ and $P_d^\sigma=P_d^\sigma$ are illustrated in Fig. 7.

IV. COMPARISONS WITH ENERGY-BAND RESULTS

The total DOS for the 14 primary bands of the perovskites is given by

$$\begin{aligned} N_t(E)&=N^\sigma(E)+N^\pi(E)\\ &=2\rho_\sigma(E)+2\rho^{\sigma^0}(E)+6\rho_\pi(E)+6\rho^{\pi^0}(E)\,. \end{aligned} \tag{135}$$

Figure 8 show a comparison of the DOS for $KTaO_3$ calculated from Eq. (135) (heavy curve) with the histogram calculated by Mattheiss.[7] The overall agreement is seen to be quite good. Some notable differences can be seen in the DOS of the σ bands between -2 and -3 eV and in the σ^* bands above 12 eV. These differences are presumed to arise from the effects of orbital symmetries not present in our model and from distant-neighbor interactions. Comparable agreement is found for $SrTiO_3$ and $NaWO_3$ (Ref. 9).

The total d-orbital PDOS and the p-orbital PDOS for the 14 bands of the perovskites is given

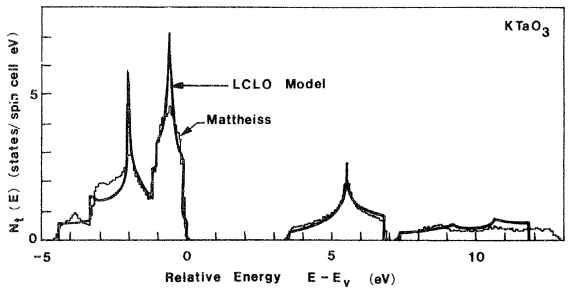

FIG. 8. Quantitative comparison of the DOS with the APW calculations of Mattheiss (Ref. 7) for $KTaO_3$. The parameters used are those of Fig. 2.

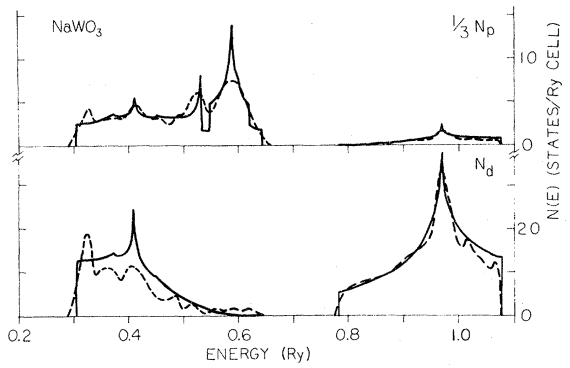

FIG. 9. Comparison of the model PDOS with the numerical results of energy-band calculations of Kopp *et al.* (Ref. 11) for $NaWO_3$. The LCLO parameters are $E_\sigma=0.54$, $E_e=1.15$, $(pd\sigma)=-0.18$, $(pp\sigma)=0.028$, $E_\pi=0.59$, $E_t=0.78$, $(pd\pi)=0.13$, and $(pp\pi)=-0.017$, all in Ry.

by

$$N_d(E)=P_d^\sigma(E)+P_d^\pi(E)\ , \tag{136}$$

$$N_p(E)=P_p^\sigma(E)+P_p^\pi(E)\ . \tag{137}$$

Figure 9 shows a comparison of $N_d(E)$ and $N_p(E)$ [calculated from Eqs. (136) and (137)] with the numerical results of Kopp *et al.*,[6] for $NaWO_3$. The overall agreement is again quite good. Some significant differences can be seen in the region of the σ band between 0.3 to 0.5 Ry in N_d. In previous works the DOS and PDOS functions described here have been employed to analyze the optical properties of $SrTiO_3$,[7] the UPS (ultraviolet photoelectron spectroscopy), and XPS spectrum of $SrTiO_3$, (Ref. 17) and the XPS spectrum of Na_xWO_3.[17]

V. SUMMARY

In the previous sections we have developed simple analytical expressions for representing the DOS and PDOS functions of the cubic d-band perovskites in terms of a few electronic parameters. The nine π bands are characterized by five parameters: E_t, E_π, $(pd\pi)$, $(pp\pi)$, and $(pp\sigma)$. The five σ bands are characterized by three additional parameters: E_e, E_σ, and $(pp\sigma)$. Thus, the 14 primary energy bands, their wave functions, DOS, and PDOS are characterized completely in terms of eight parameters. These parameters can be obtained by direct calculation. For example, calculation of the band energies at Γ, X, and R, or Γ, M, and R is sufficient to determine all electronic parameters. The model may then be used as an interpolation scheme for determining the energy bands, and wave functions at any point in the Brillouin zone and the DOS and PDOS are immediately known.

A more qualitative approach can also be used. The energies E_t, E_e, E_π, and E_σ can be approximately determined from ionization potentials and Madelung potentials.[2] The interactions can be caluclated approximately by using atomic or ionic orbitals[2,24] to calculate the transfer integrals.

An alternate use of the model is to use experimental data to determine the parameters.[17] This approach allows an approximate determination of the energy bands directly from experimental data. The utility and validity of the results derived here have been demonstrated here and in previous papers concerning the analysis of optical[7] and photoelectron[17] data of the perovskites.

ACKNOWLEDGMENTS

The authors wish to express their thanks to Dr. L. F. Mattheiss and to Dr. B. N. Harmon for supplying detailed density-of-states data from their calculations. This work was supported in part by a grant from the National Science Foundation.

*On leave from Middle East Technical University, Ankara, Turkey.

[1]L. F. Mattheiss, Phys. Rev. B 6, 4718 (1970); 2, 3918 (1970); 6, 4718 (1972).
[2]T. Wolfram, E. A. Kraut, and F. J. Morin, Phys. Rev. B 7, 1677 (1973).
[3]T. F. Soules, E. J. Kelley, D. M. Vaught, and J. W. Richardson, Phys. Rev. B 6, 1519 (1972).
[4]P. Pertosa and F. M. Michel-Calendini, Phys. Rev. B 17, 2011 (1978).
[5]W. A. Kamitakahara, B. N. Harmon, J. G. Taylor, L. Kopp, H. R. Shanks, and J. Rath, Phys. Rev. Lett. 36, 1393 (1976).
[6]L. Kopp, B. N. Harmon, and S. Liu, Solid State Commun. 22, 677 (1977).
[7]T. Wolfram, Phys. Rev. Lett. 29, 1383 (1972).
[8]F. J. Morin and T. Wolfram, Phys. Rev. Lett. 30, 1214 (1973).

[9]S. Ellialtioglu and T. Wolfram, Phys. Rev. B 15, 5909 (1977); 18, 4509 (1978).
[10]M. Cardona, Phys. Rev. 140, A651 (1965).
[11]K. W. Blazey, Phys. Rev. Lett. 27, 46 (1971).
[12]F. L. Battye, H. Hochst, and A. Goldman, Solid State Commun. 19, 269 (1976).
[13]G. K. Wertheim, L. F. Mattheiss, M. Campagna, and T. P. Pearsall, Phys. Rev. Lett. 32, 997 (1974).
[14]M. Campagna, G. K. Wertheim, H. R. Shanks, F. Zumsteg, and E. Banks, Phys. Rev. Lett. 34, 738 (1975).
[15]J. N. Chazalviel, M. Campagna, G. K. Wertheim, and H. R. Shanks, Phys. Rev. B 16, 697 (1977).
[16]V. E. Henrich, G. Dresselhaus, and H. J. Zeiger, Phys. Rev. B 17, 4908 (1978).
[17]T. Wolfram and S. Ellialtioglu, Phys. Rev. B 19, 43 (1979).
[18]J. B. Goodenough, in *Progress in Solid State Chemistry,* edited by H. Reiss (Pergamon, Oxford, 1971).
[19]J. C. Slater and G. Koster, Phys. Rev. 94, 1498 (1954).
[20]P.-O. Löwdin, J. Chem. Phys. 18, 365 (1950).
[21]L. Van Hove, Phys. Rev. 89, 1189 (1953).
[22]J. C. Phillips, Phys. Rev. 104, 1263 (1956).
[23]P. F. Byrd and M. D. Friedman, *Handbook of Elliptic Integrals for Engineers and Scientists,* 2nd ed., revised (Springer, Berlin, 1971).
[24]A. H. Kahn and A. J. Leyendecker, Phys. Rev. 135, A1321 (1964).